Fast Radiometric Compensation for Nonlinear Projectors

Matthew Post — University of Waterloo, Waterloo, Canada
Paul Fieguth — University of Waterloo, Waterloo, Canada
Mohamed A. Naiel — University of Waterloo, Waterloo, Canada
Zohreh Azimifar — Shiraz University, Shiraz, Iran
Mark Lamm — Christie Digital Systems Canada Inc., Kitchener, Canada
Email: {mpost, pfieguth, mohamed.naiel, azimifar}@uwaterloo.ca, mark.lamm@christiedigital.com

Abstract

Radiometric compensation can be accomplished on nonlinear projector-camera systems through the use of pixelwise lookup tables. Existing methods are both computationally and memory intensive. Such methods are impractical to be implemented for current high-end projector technology. In this paper, a novel computationally efficient method for nonlinear radiometric compensation of projectors is proposed. The compensation accuracy of the proposed method is assessed with the use of a spectroradiometer. Experimental results show both the effectiveness of the method and the reduction in compensation time compared to a recent state-of-the-art method.

1 Introduction

Radiometric compensation is the process of altering the output of images on a display to compensate for non-uniformity of the display. In the case of data projectors, this non-uniformity can be a product of non-uniformity of both the light source and of the projection surface. Radiometric compensation aims to achieve a more accurate representation of the projected image by modelling the non-uniformity of the system. In projector-camera systems, the camera provides the feedback required to allow the projector image to be compensated for background texture of a projection surface. In the vast majority of these systems, cameras and projectors use three-channel RGB representation of images.

In the literature, several methods for radiometric compensation have been proposed and have been shown to work effectively in real-time with linear projectors [1–3]. In general, such methods work by determining a multi-channel linear model of the reflected light for each pixel and determining the inverse solution. To create a closed calibration loop for each pixel on a given projection surface, pixel correspondences are first calculated between the projector and camera through the use of structured light in a set of training images. Next, colour training images are projected on the surface and captured with the camera. These training images are then used to constrain the solution to the system inverse model for each pixel. The result is a 3×3 matrix model V for each pixel. Let C and P denote a 3×1 vector of RGB values output from the camera and input of the projector, respectively. The inverse solution to a given system provides the required projector output, P, from a desired camera colour as follows:

$$C = VP, \quad P = V^{-1}C \tag{1}$$

This model of a pixel's colour in a projector-camera system does not include parameters for ambient light, and thus can only model systems where the projector is the only source of light for the camera. This was improved by Yoshida *et al.* [4] with the augmentation of the matrix equation with a constant term to include ambient light contributions as follows:

$$P = KC_a, \quad C_a = \begin{bmatrix} c_r \\ c_g \\ c_b \\ 1 \end{bmatrix} \tag{2}$$

where K is a 3×4 matrix that represents the inverse of the pixel colour response. Alternatively, certain projectors have nonlinear responses to inputs which prevent simple linear system modeling. The nonlinearity of the projector causes the radiometric response of each projected pixel to become nonlinear. Recently, Grundhöfer and Iwai [5] proposed a method for radiometric compensation of such non-linear systems using a lookup table per pixel and thin plate spline interpolation to approximate the colour inverse problem. The lookup table inherently provides solutions for nonlinear projector response and ambient light. However, this method has two significant drawbacks; firstly, the sparse lookup table of each pixel's colour response must be stored, and secondly, a spline interpolation must be performed for each pixel in each image to be compensated. This requires a significant increase in both computations and storage per pixel over the linear solution.

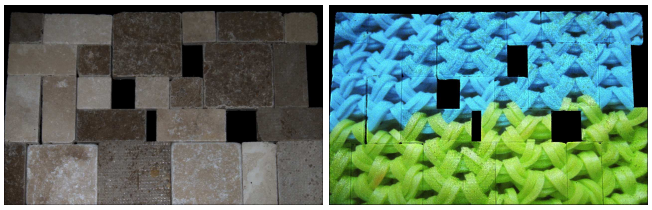

(a) *(b)*

Figure 1: (a) Sample *Stone Tile* test background and (b) compensated image using the proposed scheme. This experiment is conducted in high ambient light conditions.

In this paper, a method that efficiently computes the radiometric compensation of a nonlinear projector system is proposed. This method separates the nonlinearity of the projector from the linear radiometric compensation. The proposed scheme provides a significant reduction in computational complexity and storage requirements of the compensation when compared to that of the method in [5]. This reduction is achieved without sacrificing the accuracy of the compensation; a sample of this nonlinear compensation can be seen in Figure 1, where a stone tile wall is being illuminated with high ambient light.

2 The Proposed Scheme

Modern cinema class projectors such as the Christie Boxer and D4KLH60 operate at a resolution of 4K (4096×2160) and frame rates of 120Hz. These projectors require more computationally efficient nonlinear compensation methods than those that previously exist [5, 6]. In this section, a method capable of being applied to these high-performance cinema projectors is introduced. The proposed method uses a single lookup table to linearize the projector response, rather than using a lookup table per pixel as in [5]. The proposed method then employs the linear formulation proposed by Yoshida *et al.* [4] which uses 3×4 matrices to model the linear radiometric response of a camera to both a projector and constant ambient light sources. The linearization step in the proposed scheme therefore does not need to be calculated for each pixel, but rather for the light source and then applied to the linear response model of all pixels.

Background Modeling: Let us assume that the the screen can be modelled by Lambertian reflectance [7]. Thus, the screen irradiance for a given projector primary channel is a product of both the given pixel intensity for that channel and the spectral response of the same channel. The nonlinearity of the projector output can be caused by additional colour channels in the projector which do not directly correspond to RGB, such as cyan, magenta or white. This can also be caused by nonlinear gain applied to the colour channels such as a gamma function. Given the wavelength distribution $w_i(\lambda)$ of each colours channel i, the combined nonlinear irradiance e_i can be expressed as:

$$e_i = F_i(P(\overline{u})) \cdot w_i(\lambda) \tag{3}$$

where $\overline{u}$ is the pixel indices (u, v) in the projector frame of reference, and $F_i(\cdot)$ is the nonlinear projector response to input $P(\overline{u})$.

The background compensation for the projector is calibrated based on the colour feedback from the camera in the system. When the projector stimuli and camera responses can be treated as linear with respect to one another, the system and its inverse can be modelled as shown in (2). The colour and texture of the background surface for each pixel provide a simple scalar gain to each colour channel component, and so the system with background colouration and the corresponding compensation (the system inverse) can also be modelled as such. This linear radiometric compensation

solution can thus be applied to a non-linear system if the correct linearization of the projector is known. Let the response of the camera C to a coloured surface illuminated by a projector with a nonlinear function, $F(\cdot)$, applied to the input be represented as:

$$C = VF(P) \tag{4}$$

Then, the compensation of the system can be accomplished by inverting the system to solve for the projector intensities as:

$$\boxed{P = F^{-1}(KC_a)} \tag{5}$$

It is shown that this equation is fundamental for fast nonlinear radiometric compensation; the linear compensation matrix K is separable from the projector linearization function $F^{-1}(\cdot)$. The linear compensation method in (2) can then be used when a suitable model of $F^{-1}(\cdot)$ is known, which can in fact be learned.

The full system is then solved for each pixel by using an initial set of eight projected flat colour test patterns using the pseudo-inverse. The test patterns consist of white, the projector primaries and secondaries, and black. In the case of solving the linear system for each pixel, more test colours provides greater stability to the solution of K. The vertices of the projector's gamut were selected to improve solution stability, but the system can be solved with just the projector's primaries and a black level image.

Projector Modeling: The nonlinearity function $F(P)$ of a given projector is modelled through the use of a single lookup table to linearize the colour response for the projector. The lookup table of the proposed scheme is generated by sparsely sampling the projector's output over the full range of the projector's RGB channel inputs as follows. Single colour images are first projected on a near white surface, and captured with the camera. The camera images are then averaged over a 200×200 patch in the center of the projected field. Due to the differences of the response of the camera with respect to the stimulus of the projector, a meaningful inverse of the system must provide the projector response only in terms of projector RGB input. The solution of the projector inverse model should thus be invariant to the camera response. To achieve this, all of the sample colours as seen by the camera are remapped with respect to the projector primaries, in this case the maximum outputs of red, green and blue channels. This mapping is computed by taking the inverse of the appended RGB camera responses V_0 to projector primaries as follows:

$$P_{out} = V_0^{-1}C \tag{6}$$

$$= V_0^{-1}V_0F(P_{in}) \tag{7}$$

$$= F(P_{in}) \tag{8}$$

$$\text{where} \quad V_0 = \begin{bmatrix} v_{RR} & v_{RG} & v_{RB} \\ v_{GR} & v_{GG} & v_{GB} \\ v_{BR} & v_{BG} & v_{BB} \end{bmatrix} \tag{9}$$

and P_{out} is the nonlinear projector RGB output, C and P_{in} are the camera response and the projector RGB input in (4), and v_{ij} is the response of camera channel i to stimulus of projector channel j at maximum intensity. As shown in equations (6)-(8), the projector nonlinearity function $F(\cdot)$ can be obtained by evaluating (6). The matrix in (9) is then used to map all colours seen by the camera to a colourspace of which the projector primaries are basis vectors.

The mapped colours are thus projector outputs P_{out} in terms of projector primaries, with known input RGB vectors P. This known relationship between inputs and outputs of the projector allows a lookup table to be built with no further dependence on the camera response but is solely a product of the projector configuration. This lookup table can be built from either dense or sparse sampling, with a suitable interpolation being performed prior to radiometric compensation. In the case of sparse sampling, the projector gamut can be sampled at a subset of the possible RGB inputs, and interpolated to derive the desired lookup table. In this paper, linear interpolation with sample points chosen on a uniform 3D grid is used, resulting in n^3 points.

Background Compensation: To project a given target image on a given surface, radiometric compensation must be applied to each pixel. The compensation for a given projector and projection surface is performed by computing (5) for each desired pixel colour C in the input image. From (6) the linearization function $F^{-1}(\cdot)$ is approximated via a lookup table, and is computed once per projector configuration. The pixelwise linear compensation K can be obtained from (2) once for each projector-background setup. The evaluation of the proposed compensation method in (5) requires only a $(3 \times 4) * (4 \times 1)$ matrix multiplication and a single indexing operation per pixel in each projected frame. Comparatively, the existing state-of-the-art method in [5] requires a thin plate spline interpolation of 6^3 points per pixel.

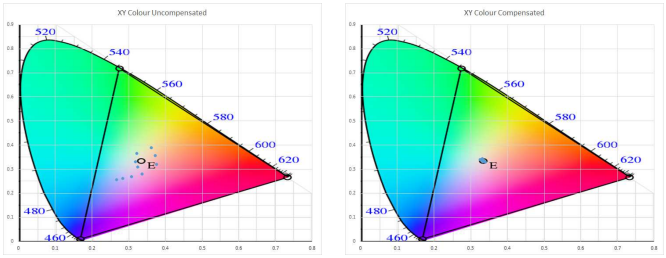

(a) (b)

Figure 2: XY measurements of (a) uncompensated and (b) compensated images.

Table 1: Comparison of ΔE colour differences for the proposed method for a white target image.

Background Colour	Red	Green	Blue	Cyan	Magenta	Yellow
Uncompensated	73.26	112.13	125.55	113.50	112.41	110.88
Proposed Method	4.40	3.01	2.36	5.13	2.28	2.36

3 Experimental Results

In order to evaluate the proposed method, it was applied to a projector-camera system comprising a Christie G Series proejector and a Point Grey Flea3 camera. The radiometric compensation accuracy is first evaluated by measuring the spectrum returning from the screen at given target points by the use of a SpecBos 1211 spectroradiometer. This radiometer is outside the calibration loop for the purposes of deriving the compensation. Then, the colour is measured in XY colour space and compensation error is computed using CIE ΔE [8] differences from a set of target colours. For evaluation, seven selected flat field target colours are used, namely, white, red, green, blue, cyan, yellow and magenta flat fields. The use of flat colours allowed the spectroradiometric measurements to be taken over a consistent target colour with only the background varying. Similarly, the printed background includes a series of saturated coloured regions, each either a primary, secondary or tertiary ink colour. The spectral measurements can then be taken on flat patches of the most difficult background colours. Figure 2 shows the XY colours obtained from the radiometer before and after compensation for a white image. The radiometric compensation not only reduced the size of the point cluster, but also correctly centred the cluster on the whitepoint $(\frac{1}{3}, \frac{1}{3})$. The ΔE for six of the colour background patches can be seen in Table 1, where the colours on the *Rainbow* background were measured with a spectrometer before and after compensation. From this, the ΔE differences were computed for both the compensated and uncompensated colours with a white target colour. Capturing the differences of the background prior to compensation provides an objective measurement of the difficulty of the background compensation scenario. From Table 1 it can be seen the ΔE error is less than 5.13 for all target colours, comparable to the median error shown on nonlinear projectors in [5]. This is consistent with the results shown in Figure 3, from which the accuracy is evident.

Figure 3 illustrates sample qualitative results of the proposed scheme on three challenging backgrounds, with six different texture patterns. The first column shows the *White Field* image projected on the *Rainbow* background. This is one of the most challenging target images for a compensation scheme, as the human eye is able to contrast opposing colours and even a slight deviation from perceived white is immediately apparent. Furthermore, any textures and edges present in the compensated image are extremely evident. The proposed method compensates reasonably well, yet the underlying colours can be seen. The second column shows the *Swirl* image projected on the *Rainbow* background. The *Swirl* has a variety of smooth coloured regions which maintain a single hue across colour boundaries of the *Rainbow* background. If any target colour is compensated differently on two background colours, an edge becomes evident as in the thirds row. The *Blanket* test image provides the challenge of compensating a high-contrast monochromatic image for all colours of the *Rainbow* background. Similar to the *White Field*, any deviation from white in the *Blanket* is evident,

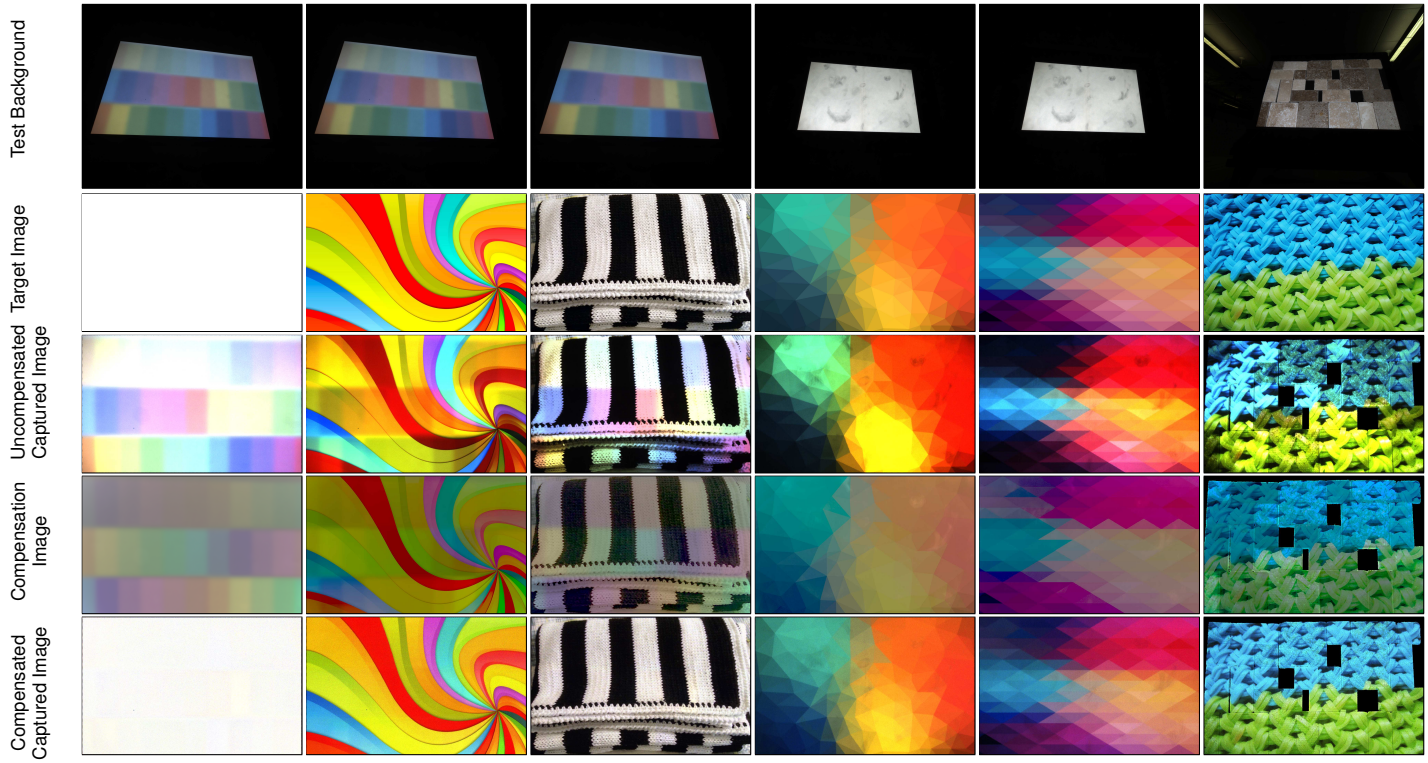

Figure 3: Qualitative results of the proposed scheme on *Rainbow* (1st, 2nd and 3rd columns), *Smudged* (4th and 5th columns) and *Stone Tile* (6th column) backgrounds using six different test images, namely, from left to right, *White Field*, *Swirl*, *Blanket*, *Geometric-1*, *Geometric-2* and *Weave*. Note: black borders are not part of the images.

Table 2: Comparison of the memory and the time complexities of the proposed scheme and the method in [5], where bold denotes the best performance and * denotes a calculated figure.

Method	Memory (GiB)			Time, CPU (s)		
	720p	1080p	4K	720p	1080p	4K
Grundhöfer & Iwai [5]	2.50*	-	-	7.1	-	-
Proposed Method	**0.46**	**0.56**	**1.1660**	**0.53**	**0.817**	**2.1**

and very bright and dark regions must be compensated simultaneously. Columns four and five show *Geometric* target images on the *Smudge* background, similar to a poor cinema screen. The *Geometric* images include a variety of colours without high frequency texture to hide the background. The final column shows a colourful *Weave* pattern on a *Stone Tile* background. This compensation scenario is the most difficult compared to the other situations for four reasons: the surface is not smooth or even continuous; the surface includes black and highly specular regions; there is a fine texture to each tile of the surface and this scene was recorded with full fluorescent ambient light in the room. As seen in the last row of Figure 3, these situations are all effectively compensated by the proposed scheme from the perspective of the camera.

To evaluate the efficiency of the proposed scheme, both this method and the method in [5] are evaluated at three different resolutions, namely, 720p, 1080p and 4K, and the results are shown in Table 2, where dashes in Table 2 indicate the method could not be run at the specified resolution. In this comparison, the computational performance of the proposed method was assessed using a modern CPU[1]. Table 2 shows the improvements made by the proposed method over the state-of-the-art method in [5], including more than 80% reduction in memory, and more than 13 times reduction in computation time, with more performance gains at larger resolutions.

4 Conclusions

In this paper, the design and evaluation of a new method for real-time nonlinear radiometric compensation has been presented. The proposed method solves the nonlinear radiometric compensation problem by separating the linearization problem from that of linear radiometric compensation. Experimental results have shown that the proposed scheme has allowed compensation to be applied with a fraction of the memory and computational requirements than that achieved by a recent state-of-the-art method. Additionally, the proposed scheme has offered a very low compensation error when evaluated by a sensor outside of the compensation feedback loop. Compensation of an adverse multi-coloured background was accomplished with a maximum error of 5.13 over the field of the image. This work will be extended to video applications, and to eliminate the dependence on camera colour response for the final compensation.

[1] A CPU with 4 cores operating at 3.40GHz was used.

5 Acknowledgments

We would like to thank the Ontario Centres of Excellence - Voucher for Innovation and Productivity II (OCE-VIP II), the Natural Sciences and Engineering Research Council of Canada - Collaborative Research and Development (NSERC-CRD) and Christie Digital Systems for sponsoring this research work.

References

[1] S. Mihara, D. Iwai, and K. Sato, "Artifact reduction in radiometric compensation of projector-camera systems for steep reflectance variations," *IEEE Transactions on Circuits and Systems for Video Technology*, vol. 24, no. 9, pp. 1631–1638, 2014.

[2] O. Bimber, D. Iwai, G. Wetzstein, and A. Grundhoefer, "The visual computing of projector-camera systems," *Computer Graphics Forum*, vol. 27, no. 8, pp. 2219–2245, 2008.

[3] S. K. Nayar, H. Peri, M. D. Grossberg, and P. N. Belhumeur, "A projection system with radiometric compensation for screen imperfections," in *Columbia University Technical Report*, 2003.

[4] T. Yoshida, C. Horii, and K. Sato, "A virtual color reconstruction system for real heritage with light projection," in *Proc. International Conference on Virtual Systems and Multimedia*, 2003, pp. 1–7.

[5] A. Grundhöfer and D. Iwai, "Robust, error-tolerant photometric projector compensation," *IEEE Transactions on Image Processing*, vol. 24, no. 12, pp. 5086–5099, 2015.

[6] A. Grundhöfer, "Practical non-linear photometric projector compensation," in *Proc. IEEE Conference on Computer Vision and Pattern Recognition Workshops*, June 2013, pp. 924–929.

[7] S. J. Koppal, *Lambertian Reflectance*, K. Ikeuchi, Ed. Boston, MA: Springer US, 2014.

[8] G. Sharma, W. Wu, and E. N. Dalal, "The ciede2000 color-difference formula: Implementation notes, supplementary test data, and mathematical observations," *Color Research & Application*, vol. 30, no. 1, pp. 21–30.